

THE SOLUTION OF 3-DIMENSIONAL INDUCTION HEATING PROBLEMS
USING AN INTEGRAL EQUATION METHOD

W. R. Hodgkins and J. F. Waddington

Abstract - The boundary integral equation method is applied to the solution of the induction heating of three dimensional objects. Two methods are explored. The first uses a direct solution of the electric field integral equation and the second uses a combination of the electric and magnetic equations and represents the tangential components of the surface electromagnetic field by three scalar surface potentials. Both fields and potentials are given a finite element representation. Results for some simple cases are considered.

INTRODUCTION

The aim of this work is to provide a tool to assist in the design of induction heating devices both for metal melting and billet reheating. Programs already exist [1,2] and are used extensively in cases where the problems may be treated as two dimensional but many instances arise where it is desirable to be able to analyse the full three dimensional geometry. For example, considerable work has been carried out at E.C.R.C. on designing highly efficient induction heaters for billets of various geometries with the aim of minimising energy usage whilst producing a highly controlled heat treatment: the channel furnace, where the molten metal is inductively heated in a loop, resembling a handle on a cup or inverted suitcase, is a case where it is almost impossible to make sensible two dimensional approximations.

An earlier study [3] surveyed a number of possible methods for solving these problems. Amongst those considered were finite difference and finite element methods using various formulations for potential or field variables, integral equation techniques, and hybrid methods using an integral equation for the far field and a partial differential equation for the near field. It concluded that for treating problems where the electromagnetic properties of the material being heated are relatively uniform a version of the integral equation method offered considerable promise. This assumption is generally valid when molten metal is being heated, but is not normally true, for example, when magnetic materials are being heated through the Curie point. For regions of uniform material the three dimensional integral equation may be reformulated to give an integral equation over the surface of the body, thus effectively reducing the problem to two dimensions.

GOVERNING EQUATIONS

The basic equations for the boundary integral equation method were derived by Stratton and Chu [4] and have been examined in considerable detail by Müller [5]. For typical induction heating problems at low or medium frequency the equations are slightly simplified by making the usual assumption that the displacement currents may be neglected in comparison with the conduction currents and ignoring the transient components of the fields. Maxwell's equations then have the simplified form:

$$\nabla \wedge \underline{H} = \underline{J} + \underline{J}_0 = \sigma \underline{E} + \underline{J}_0 \quad \nabla \wedge \underline{E} = -i\omega \mu \underline{H} \quad (1)$$

where the magnetic and electric fields have the form $\underline{H}_{\text{exp}}(i\omega t)$ and $\underline{E}_{\text{exp}}(i\omega t)$ respectively, and where source currents \underline{J}_0 only exist in the non-conducting regions where $\sigma = 0$.

Consider now a homogeneous conducting region V bounded by the closed surface S with outward normal \underline{n} . The usual integral equations for the fields within V are:

$$\underline{H}(\underline{r}') = -\frac{1}{4\pi} \int_S [\underline{n} \wedge \underline{E}(\underline{r}) \underline{U} + (\underline{n} \wedge \underline{H}(\underline{r})) \wedge \nabla \underline{U} + (\underline{n} \cdot \underline{H}(\underline{r})) \nabla \underline{U}] dS \quad (2)$$

$$\underline{E}(\underline{r}') = -\frac{1}{4\pi} \int_S [-i\omega \mu \underline{n} \wedge \underline{H}(\underline{r}) \underline{U} + (\underline{n} \wedge \underline{E}(\underline{r})) \wedge \nabla \underline{U}] dS \quad (3)$$

where:

$$\underline{U}(\underline{r}, \underline{r}') = \exp(-ik|\underline{r} - \underline{r}'|) / (|\underline{r} - \underline{r}'|) \quad k^2 = -i\omega \mu \sigma \quad (4)$$

Here the assertion that $\underline{n} \cdot \underline{E}$ is zero at the surface has been used to delete the corresponding term from the usual form of the integral equation. Note that the equations for \underline{E} and \underline{H} are not independent since each is the curl of the other. The corresponding equations for the external region with zero conductivity, permeability μ and source currents \underline{J}_0 are:

$$\underline{H}(\underline{r}') = 2\underline{H}_0(\underline{r}') + \frac{1}{4\pi} \int_S [(\underline{n} \wedge \underline{H}(\underline{r})) \wedge \nabla \underline{U}_0 + (\underline{n} \cdot \underline{H}(\underline{r})) \nabla \underline{U}_0] dS \quad (5)$$

$$\underline{E}(\underline{r}') = 2\underline{E}_0(\underline{r}') + \frac{1}{4\pi} \int_S [-i\omega \mu \underline{n} \wedge \underline{H}(\underline{r}) \underline{U}_0 + (\underline{n} \wedge \underline{E}(\underline{r})) \wedge \nabla \underline{U}_0] dS \quad (6)$$

where \underline{n} is now the internal normal to the external region, $\underline{U}_0 = 1/|\underline{r} - \underline{r}'|$ and the source fields \underline{H}_0 and \underline{E}_0 are given by:

$$\underline{H}_0(\underline{r}') = \frac{1}{4\pi} \int_V \underline{J}_0 \wedge \nabla \underline{U}_0 \, dV \quad \underline{E}_0(\underline{r}') = \frac{1}{4\pi} \int_V i\omega \mu \underline{J}_0 \underline{U}_0 \, dV \quad (7)$$

The above equations for the fields in the internal and external regions may be used to give the fields at the surface S if the factor 4π is replaced by the factor 2π in (2), (3), (5) and (6), and the Cauchy principal value of the integral is used for the terms $(\underline{n} \wedge \underline{H}(\underline{r})) \wedge \nabla \underline{U}$ and $(\underline{n} \wedge \underline{E}(\underline{r})) \wedge \nabla \underline{U}$. In the derivation of these equations it is generally assumed that the surface S is smooth and that the tangential components of the electromagnetic field are continuous with continuous first derivatives.

Since the normal component of magnetic field, $\underline{n} \cdot \underline{H}$, may be expressed in terms of the surface derivatives of $\underline{n} \wedge \underline{E}$ it is possible to use one or a combination of the external equations, (5) and (6), in conjunction with one or a combination of the internal equations, (2) and (3), to determine the tangential fields at the surface and hence the fields everywhere. Various combinations of the equations have been suggested by Poggio and Miller [6] and considerable experience has been gained of the value of different formulations as applied to the related problem of antennae design [7]. In the present work two formulations have been used. The first is to work solely with the electric field equations, (3) and (6). This has the advantage that no normal components of the fields now appear in the equations and hence the use of derivatives of the tangential fields is avoided. The second approach is to use the form proposed by Müller [5]. This is an appropriate combination of the internal and external equations for which Müller has demonstrated uniqueness and convergence. In the particular case of low frequency current and a non-conducting external region these become the equation for the internal electric field and the sum of the magnetic field equations

The authors are with the Electricity Council Research Centre, Capenhurst, Chester, England, CH1 6PS.

weighted by the permeability of each region. i.e.

$$(\mu + \mu_0) \underline{n} \cdot \underline{H}(\underline{r}') = 2\mu_0 \underline{n} \cdot \underline{H}_0(\underline{r}') - \frac{D}{2\pi} \int [\mu \sigma \underline{n} \cdot \underline{E}(\underline{r}) \underline{U} + (\underline{n} \cdot \underline{H}(\underline{r}))_\Lambda (\mu \underline{V} \underline{U} - \mu_0 \underline{V} \underline{U}_0) + (\underline{n} \cdot \underline{E}(\underline{r})) (\underline{V} \underline{U} - \underline{V} \underline{U}_0)] dS \quad (8)$$

NUMERICAL METHOD

The finite element method was chosen to discretise the integral equations. This in principle allows a choice in the level of approximation and in element shape. The present work was limited to plane triangular elements and uniform fields in each element. Since the integral equations give values at a point whereas the fields are valid over an element, a further integral was carried out over each element to give the appropriate average. This also had the value that it reduced the weight of the value of the integral at nodes and sharp edges where the value of the approximations may be indeterminate or changing rapidly.

For the method based on the electric fields the set of linear equations is then set up directly from the two equations:

$$\underline{n} \cdot \underline{E}(\Delta j) = -\frac{1}{2\pi \Delta j} \iint \underline{n}' \cdot [-i\omega \mu \underline{n} \cdot \underline{H}(\underline{r}) \underline{U} + (\underline{n} \cdot \underline{E}(\underline{r}))_\Lambda \underline{V} \underline{U}] dS \cdot d\Delta j \quad (9)$$

$$\underline{n} \cdot \underline{E}(\Delta j) = 2\underline{n} \cdot \underline{E}_0(\Delta j) + \frac{1}{2\pi \Delta j} \iint \underline{n}' \cdot [-i\omega \mu_0 \underline{n} \cdot \underline{H}(\underline{r}) \underline{U}_0 + (\underline{n} \cdot \underline{E}(\underline{r}))_\Lambda \underline{V} \underline{U}_0] dS \cdot d\Delta j \quad (10)$$

which provides two independent equations for the tangential component of electric field for each triangle j of area Δj . The unknown tangential electric and magnetic fields are then determined by a direct solution of the set of linear equations.

For the method based on Müller's equations some further refinements were introduced. First in order to avoid representing surface vectors directly, the tangential electric and magnetic fields at the surface are represented as derivatives of surface scalar potentials [8]. This has the advantage of providing a much simpler scalar representation. Also, since in the present case the exterior region is non-conducting, the magnetic field at the surface requires only one potential. Thus the expressions for the tangential surface fields are:

$$\underline{n} \cdot \underline{H} = \underline{n} \cdot \underline{V}_s \phi \quad \underline{n} \cdot \underline{E} = \underline{n} \cdot \underline{V}_s \xi + \underline{V}_s \eta \quad (11)$$

where \underline{V}_s is the surface vector operator defining the surface gradient [5,7] and is also used to operate on a vector to form the surface divergence. i.e.

$$\underline{V}_s \phi = \underline{V} \phi - (\underline{n} \cdot \underline{V} \phi) \underline{n} \quad \underline{V}_s \underline{u} = \underline{V} \underline{u} - \frac{\partial}{\partial n} (\underline{n} \cdot \underline{u}) \quad (12)$$

On a simply connected closed surface where a field is defined by a pair of potentials, the potentials are continuous and unique to within a constant term. For multiply connected surfaces it is necessary to introduce appropriate cyclic potentials. Thus for a doubly connected region, such as a torus, both ξ and η may be regarded as cyclic potentials with a single period, or alternatively the same vector field may be derived by making either ξ or η doubly periodic. This is especially convenient for expressing the magnetic field, as the second potential has already been dispensed with. The two periodicity conditions imposed on ϕ are defined by:

$$\oint \underline{H} \cdot d\underline{s} = \int \underline{J} \cdot \underline{n} dS \quad (13)$$

When this condition is evaluated for any surface contour enclosing the toroidal conductor it gives the circulating current in the conductor, and when it is

evaluated round an orthogonal contour it gives the total external current threading the torus.

In order to complete the substitution of the potentials for the fields in (8) it is necessary to express the normal component of magnetic field in terms of the potentials. This can be evaluated as:

$$\underline{H} \cdot \underline{n} = i(\underline{n} \cdot \underline{V}_s \underline{E}) / \omega \mu = -i \underline{V}_s^2 \eta / \omega \mu \quad (14)$$

Rather than applying the resultant integral equations directly to evaluate the field at isolated points on the surface, it is more appropriate to obtain suitable averages for satisfying the equations approximately over the whole surface. In keeping with the finite element method the equations are integrated a second time after multiplying by two arbitrary surface scalar potential functions, $\underline{V}_s \alpha$ and $\underline{n} \cdot \underline{V}_s \beta$. The functions may then be subject to small variations following the Galerkin procedure and a set of linear equations obtained. Assuming a smooth surface and appropriate degrees of continuity of the various functions the resultant equations are:

$$(\mu + \mu_0) \int \underline{V}_s' \phi \underline{V}_s' \delta \beta dS' = 2\mu_0 \int \underline{V}_s' \phi_0 \underline{V}_s' \delta \beta dS' + \frac{1}{2\pi} \int \{ \underline{V}_s' \sigma \underline{V}_s' \delta \beta (\underline{n} \cdot \underline{V}_s' \xi + \underline{V}_s' \eta) - [\underline{V}_s' \delta \beta \Lambda (\underline{n} \cdot \underline{V}_s' \phi)] \cdot (\mu \underline{V} \underline{U} - \mu_0 \underline{V} \underline{U}_0) + i \underline{V}_s' \delta \beta \underline{V}_s'^2 \eta (\underline{U} - \underline{U}_0) / \omega \} dS \cdot dS' \quad (15)$$

$$\int \underline{V}_s' \xi \underline{V}_s' \delta \beta dS' = \frac{1}{2\pi} \iint \{ i\omega \mu \underline{U}' \underline{V}_s' \delta \beta (\underline{n} \cdot \underline{V}_s' \phi) - [\underline{V}_s' \delta \beta \Lambda (\underline{n} \cdot \underline{V}_s' \xi + \underline{V}_s' \eta)] \cdot \underline{V} \underline{U} \} dS \cdot dS' \quad (16)$$

$$\int \underline{V}_s' \eta \underline{V}_s' \delta \alpha dS' = \frac{1}{2\pi} \iint \{ -i\omega \mu \underline{U}' (\underline{n}' \cdot \underline{V}_s' \delta \alpha) (\underline{n} \cdot \underline{V}_s' \phi) + [(\underline{n}' \cdot \underline{V}_s' \delta \alpha) \Lambda (\underline{n} \cdot \underline{V}_s' \xi + \underline{V}_s' \eta)] \cdot \underline{V} \underline{U} \} dS \cdot dS' \quad (17)$$

where the external applied magnetic potential, ϕ_0 , is given for closed loops of source current by:

$$\phi_0(\underline{r}') = -\frac{1}{4\pi} \int \underline{J} \cdot \underline{\Omega} dV \quad (18)$$

where $\underline{\Omega}$ is the solid angle subtended by the current loop at the point \underline{r}' .

The equations developed so far have assumed a smooth surface and the appropriate degree of continuity of the fields. However, unless an unduly fine mesh is to be used and rounded corners introduced it is important that the method is valid when the geometry includes sharp edges. Singularities of the integrand arise at sharp edges and corners but fortunately as is typical of finite element energy methods it is only necessary to determine whether there is a finite contribution to the double integrals in these circumstances. An examination of the terms shows that the only term making such a contribution is the final term of (15) involving the second derivatives of scalar potential. Stratton [4] introduces a line distribution of charge density at edges to accommodate this effect. The other terms involve the value of the fields and will only cause problems if the actual field becomes large enough for there to be a contribution to the physical field, in which case a fine mesh will be required to obtain a useful average value of the field in this neighbourhood. The term involving the second derivative of potential may be readily evaluated at an edge, since:

$$\int \underline{V}_s' \eta f(\underline{r}, \underline{r}') dS = - \int \underline{V}_s \eta n_0 f(\underline{r}, \underline{r}') dl \quad (19)$$

where \underline{n}_0 is the external normal in the plane of each neighbouring triangle to the edge l . The last term in (15) may thus be readily rewritten to include the

contribution from the edges. In the special case under consideration when the potentials and the trial functions are linear potentials, the second derivatives over the elements are zero and the only contribution from this term is the double integral over the edges which is:

$$\frac{1}{2\pi} \iint_{\Gamma} [(\nabla_s \delta p \cdot \underline{n}_s) (\nabla_s \eta \cdot \underline{n}_s) (U - U_0) / w] d\Gamma \quad (20)$$

NUMERICAL IMPLEMENTATION

One difficulty in the implementation of the integral method is that in regions where the fields may be fairly uniform and hence the use of a coarse mesh would seemingly be adequate the integrands contain functions which vary as the skin depth and hence may require a fine scale for accurate integration. Where the terms in the integrand give rise to analytic expressions which may be readily evaluated this causes no problem, but in general this is not the case and care must be taken over the numerical integration, especially as some of the integrands are singular at points on the edges of neighbouring triangles. To provide sufficient accuracy a technique was therefore devised which divides triangular elements into a regular pattern of sub-triangles which are placed into two classes of similar triangles depending upon their orientation. Numerical integrations are then performed with respect to the centroids of each set of similar triangles separately and a linear combination of the two estimates is formed to eliminate first order errors. This technique was implemented in the method based on the electric field equations so as to give integrations to different accuracies as required.

For the method based on Müller's equations the integrations were only based on the 3 point Gauss formula for each triangle and the 2 point Gauss formula for the line integrals.

The coefficients form the elements of a non-symmetric complex matrix. For a single conducting region the matrix is essentially non-sparse but for a region much larger than the skin depth many of the elements are small. The possibility of reducing the amount of computation in solving the matrix by taking advantage of the structure of the matrix has been discussed previously [3]. For the small test cases used here to evaluate the method a direct method of solution has been employed. However, some tests using the Müller method were solved by iteration as quite rapid convergence would be expected on physical grounds for problems of interest on induction heaters.

RESULTS

The aim was to choose some simple test cases where as far as possible the solution is known and then examine the numerical results to establish which factors are of most importance in determining accuracy and speed of solution. Unfortunately it is not easy to find genuine three dimensional test cases which can be readily modelled by the plane triangular elements incorporated in the present program and for which a complete solution is known. Two test cases were therefore considered.

The first is a circular cylinder with a ratio of length to radius of three where the conductivity was chosen to give a skin depth of either one or three radii. An approximate solution to this problem was calculated using a finite element program taking advantage of axial symmetry for an applied uniform magnetic field.

A number of problems became apparent from a comparison of the results. First the finite element

method itself gave results which varied by a small amount depending not only on the fineness of the mesh but more particularly upon the placing of the assumed finite external boundary containing the problem. This arises since the boundary conditions for the integral equation method are imposed in a different form than in the finite element or difference methods. Whilst this difference would not be very significant for calculating power in induction heaters where the designer is largely only interested in an overall accuracy of a few percent, it does mean that the estimates of the fields, especially the magnetic field, can vary by a few percent in both phase and magnitude. This makes evaluation of the results for the integral equation methods difficult.

A second problem is that the curved surface of the cylinder is approximated by straight sides and the results for the curved cylinder will necessarily differ from the correct, but unknown, solution of the straight sided approximation unless a very large number of sides is used. It is thus not easy to separate errors arising from an inadequate geometrical approximation from those which arise from poor accuracy in the integral equation approximation.

The results show that for the case of the low conductivity cylinder the electric field is fairly well determined in all the approximations. This is not too surprising since its major component is directly induced from the applied magnetic field. The electric field method also gives good values for the magnetic field in the regions away from the ends but the program based on the Müller method only gives the same accuracy when the cylindrical shape is well approximated. Since only a coarse integration method is used in this implementation it is not clear whether the lack of accuracy depends on the poor integration or the presence of the sharp edges which give rise in this method to explicit terms.

Although the magnetic field in the region of the ends is less well determined both in the finite element and integral equation solutions there is general agreement between the various approaches. Figure 1 shows the out of phase component of the axial magnetic field, H_z , along the curved surface for the electric field method, the Müller method, the finite element method and the asymptotic solution determined analytically for small conductivity.

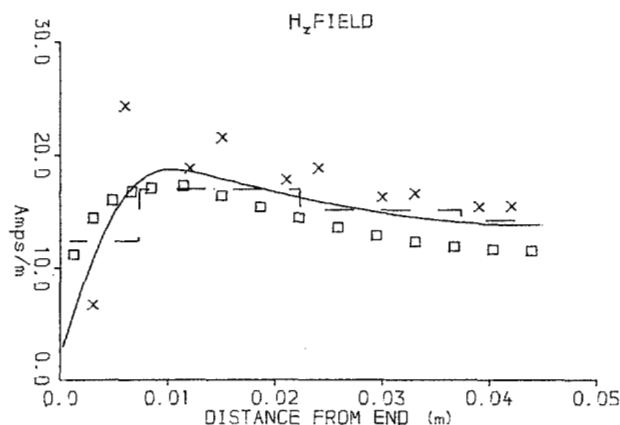


Fig. 1. H_z on curved surface of cylinder.
Low conductivity case.
— Asymptotic limit for small conductivity.
— Müller Method.
x x x Electric Field Method.
□ □ □ Finite Element Method.

The results for the electric field method show an oscillation in magnitude between neighbouring triangles lying between the same axial coordinates which reduces as the mesh is refined. In contrast the Müller method allows far less freedom to the fields which are constrained by the potentials and there appears to be a tendency to over smooth the fields.

The results for the cylinder with the higher conductivity show similar features. Table 1 lists the values on the curved surface at the centre and end planes of the circumferential component of electric field and the axial component of magnetic field.

Table 1
Fields on curved surface of high conductivity cylinder.

	E_z (mV/m)	H_z (A/m)
Centre plane		
Electric Field Method	-2.269-i3.125	1066+i28.5
Müller Method	-2.142-i3.313	1069+i43.3
Finite Element Method	-2.135-i3.076	1022+i27.9
Infinite Cylinder	-2.132-i2.955	1000
End plane		
Electric Field Method	-1.896-i4.274	1167+i85.0
Müller Method	-1.729-i3.871	1043+i86.6
Finite Element Method	-1.479-i4.304	1054+i93.4

The second test case was a Faraday Ring in the form of a square section torus of dimensions $0.01\text{m} \times 0.01\text{m}$ and inner radius 0.01m with a high conductivity, $10^8/\text{ohm.m.}$, energised by 6 or 12 windings to provide a total magnetomotive force of 10A . This problem was chosen because the surface magnetic field depends only on the applied magnetomotive force and is unchanged by the eddy currents in the ring. This gives an exact check on the surface magnetic fields obtained from the solution of the integral equations. This property also means that the torus is a true boundary value problem and reliable results could be expected from the finite element method used to generate the surface electric fields for comparison with the integral equation solution.

For this problem only the integral method using the electric field equations was tried at two different levels of geometrical approximation. The first used a coarse mesh based on a six sided approximation to the torus, Fig.2, whilst the second used a twelve sided figure, Fig.3, to provide a much finer mesh.

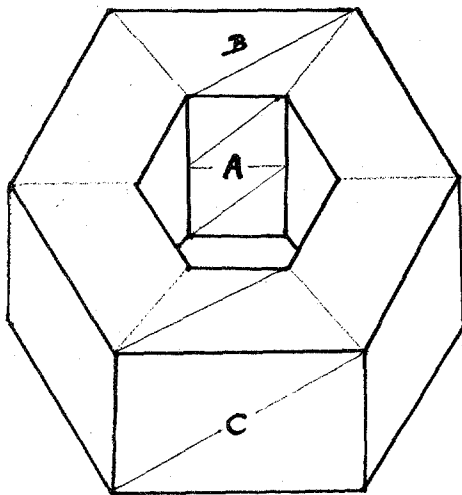


Fig 2. View of 6 sided torus.

Advantage was taken of symmetry to reduce the solution time. The coarse mesh was solved for 5 triangles and the fine mesh for 20 triangles. Thus the major part of the solution time was taken by coefficient generation.

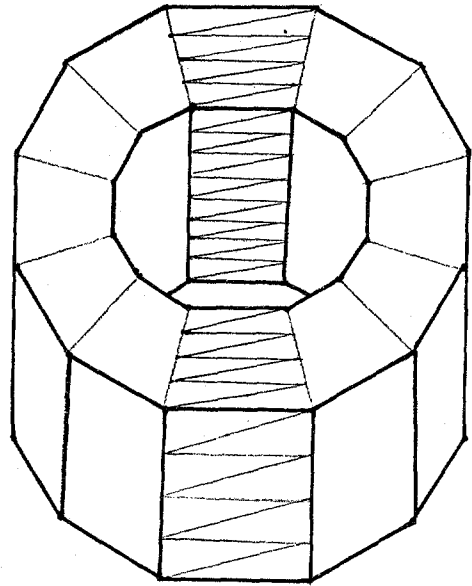


Fig. 3. View of elements of 12 sided torus.

Table 2 shows the results for the torus calculations at points on the surface labelled A,B,C on Fig.2. The tangential magnetic field, which is known exactly, and the finite element solution for the tangential electric field are shown for comparison. Results are shown for 6 and 12 sided models of the torus with three methods of applying the same magnetomotive force: a straight line current flowing along the axis of symmetry, and 6 or 12 current windings symmetrically placed around the torus. Again reasonable results are obtained in the regions away from the edges, but large errors are apparent near the edges which reduce only slowly as the mesh is refined.

Table 2
Fields on the surface of the torus.

Position:	A	B	C
Tangential Electric Field (mV/m)			
F	-0.025-i0.176	-0.021-i0.13	0.017+i0.106
B1	-0.057-i0.256	0.004-i0.005	0.015+i0.146
B2	-0.051-i0.244	0.002-i0.003	0.028+i0.159
B3	-0.1 -i0.25	-0.003-i0.047	-0.040+i0.033
B4	-0.1 -i0.25	-0.004-i0.049	-0.040+i0.033
Tangential Magnetic Field (A/m)			
F	159.2	106.1	79.6
B1	173.1+i10.9	77.8+i16.2	101.9+i8.5
B2	166.3+i10.1	6.3+i2.0	82.3+i10.1
B3	167.7+i12.6	79.8+i1.5	36.7+i6.7
B4	168.2+i12.7	80.2+i1.4	37.8+i6.8

Key: F Finite element solution for E.

Exactly known value for H

Electric field integral equation solution

B1 6 sided model, axial drive current.

B2 12 sided model, axial drive currents.

B3 6 sided model, drive current 6 windings.

B4 6 sided model, drive current 12 windings.

DISCUSSION

In general the results of the test cases show that where the surface is smooth and the fields fairly uniform there is no great difficulty in obtaining accurate answers using the integral equation methods. However, whereas in finite element methods a coarse mesh with little computation can then be used, for integral methods the integration must still be carried out, at least in the first integral, to a relatively high degree of accuracy which necessitates either a

mesh on the scale of the skin depth or a fine subdivision for the numerical integration. Where there are edges or the field is changing rapidly, and these features went together in the test cases, it is more difficult to establish accurate answers. The electric field method, as implemented here, shows strong oscillations in the magnetic field between neighbouring triangles even after using the double integral technique, although the oscillations reduce with reducing mesh size. The origin of the oscillations is not clear but could possibly be reduced by imposing additional constraints on the fields by using potentials as in the implementation of the Müller method. Because the program took advantage of symmetry it was possible to evaluate the coefficients to a high accuracy and also work with a fairly fine mesh. For example the results for the high conductivity cylinder were obtained with elements spanning each of the 12 sides of the straight sided cylinder, with the length divided into 10 equal sections and the radius divided into 3 sections at each end. This gives 182 nodes and 360 triangles. A much finer mesh for a problem not exhibiting symmetry could hardly be afforded so the best approach would appear to be to replace the constant field approximation by linear fields and to introduce curved elements to supplement the plane triangles.

The program for the Müller method did not take advantage of symmetry. The results quoted are for an 11 sided cylinder with each end divided into 2 sections and the length divided into 7 sections, giving 112 nodes and 220 triangles. Here there appeared to be a definite gain in accuracy as the mesh was refined, but much more improvement would be expected by incorporating quadratic potentials and curved elements. This would reduce the significance of the line integral arising from the normal magnetic field which with a coarse mesh is probably the major factor leading to relatively poor accuracy at the ends of the cylinder. If good values for the average fields in each element are attained then a further integral would give the variation of the fields over the elements. This has not been carried out for the present work.

In comparison with integral equation methods it should be noted that the finite element program for the cylindrical problem used 615 nodes and 1140 elements with a linear variation of vector magnetic potential within each triangular element. The outer boundaries were at a radial distance of 0.2m and an axial distance of 0.3m. A finer mesh and more distant boundaries would have been desirable but the program was already picking up oscillations in derived quantities and it was not clear that an accurate result for the magnetic field near the end of the cylinder had been achieved.

With the size of problem solved here the largest time was used in forming the matrix coefficients. This increases in proportion to the square of the number of elements, although for very large problems some of the coefficients will be negligible leading to some saving in computation. However the time for a direct solution of the matrix equations increases in proportion to the cube of the number of nodes and will eventually become an important factor. For all the test cases on the cylinder the Müller method always converged quickly using a simple iterative method. Typically the potentials converged to within about 1% in 12 iterations and to about 0.1% in 20 iterations. The form of the linear equations for the Müller method is:

$$B_0 = B_0 + C_{01} \frac{\partial}{\partial x} + C_{02} \frac{\partial}{\partial y} + C_{03} \frac{\partial}{\partial z} \quad (21)$$

$$B_1 = \dots + C_{11} \frac{\partial}{\partial x} + C_{12} \frac{\partial}{\partial y} + C_{13} \frac{\partial}{\partial z} \quad (22)$$

$$B_2 = \dots + C_{21} \frac{\partial}{\partial x} + C_{22} \frac{\partial}{\partial y} + C_{23} \frac{\partial}{\partial z} \quad (23)$$

where B is a real sparse symmetric matrix, similar to

the two dimensional Laplace equation matrix, and the C matrices are complex. For the iterative method the three matrix equations were first multiplied by B and then a Jacobi iteration without acceleration was performed. As this worked adequately more refined procedures were not investigated although they could be advantageous in solving much larger problems.

For ease of development all the calculations were carried out on a Prime 650 computer which was readily available. In view of the rapidly increasing size of the matrices as a function of the number of unknowns it is unlikely that problems more than 50% larger than the current problems could be conveniently solved on this machine. However, more powerful processors or the use of special Array Processors [3] should enable much larger problems to be solved, but to what extent these will provide accurate answers remains to be seen. The Electricity Council is sponsoring work on the measurement of the fields and forces in a model of a coreless furnace [9], and it is apparent that some considerable care must be taken both in calculation and experimental measurement even in this two dimensional case if satisfactory results are to be obtained. Thus there may be some difficulty in verifying results calculated for a genuine three dimensional problem.

CONCLUSIONS

The work here may be regarded as providing a limited demonstration of the usefulness of boundary integral methods in solving three dimensional eddy current problems. Satisfactory results are obtained for smooth surfaces but problems still remain in providing adequate representation for surfaces with sharp edges. It is unlikely that the solution will be to use a very fine mesh but alternative routes of introducing curved elements and quadratic potentials are more promising. For programs to solve problems of practical use to the engineer it will be very important to take the maximum advantage of any symmetry in the problem.

For many problems a large part of the work is in evaluating the coefficients involving surface integrals and it is important that ways to minimise this task are developed. For large problems when the solution time may become dominant it is encouraging that the method based on Müller's equations showed good convergence.

REFERENCES

- [1] Hodgkins W.R. Mathematical calculations on electromagnetic stirring. ECRC/MM12 1972.
- [2] Gibson R.C. A computer method of calculating the eddy current heating of magnetic materials, with a comparison between predicted and measured results in a 2MVA induction furnace. COMPUMAG 1976.
- [3] Cross A.D., Hodgkins W.R., Waddington J.F. The computation of three dimensional electromagnetic fields: A feasibility study. ECRC/M1198 1978.
- [4] Stratton J.A. Electromagnetic Theory. McGraw Hill, New York 1941.
- [5] Müller C. Foundations of the mathematical theory of electromagnetic waves. Springer Verlag 1969.
- [6] Poggio A.J., Miller E.K. Integral equation solutions of three dimensional scattering problems. (In 'Computer techniques for electromagnetics.' Pergamon 1973)
- [7] Jones D.S. Methods in Electromagnetic Wave Propagation. Oxford University Press, 1979.
- [8] Rham de G. Variétés différentiables. Hermann, Paris, 1960.
- [9] Moore D.J., Hunt J.C.R. Electromagnetic Stirring in the Coreless Induction Furnace. Proc. 3rd. Beer-Sheva Symposium on MHD Flows and Turbulence. Israel Universities Press.